Acta Mechanica 155, 203–214 (2002)

ACTA MECHANICA

A screw dislocation interacting with inclusions in fiber-reinforced composites

Z. M. Xiao and **B. J. Chen,** Singapore

(Received April 24, 2001)

Summary. A closed-form analytical solution is given for the stress field due to a screw dislocation interacting with nearby inclusions (the fibers) in a fiber-reinforced composite material. The dislocation is assumed near one of the inclusions, while the influence of other surrounding inclusions on the dislocation is taken into consideration through the three-phase composite cylinder model. The formulation procedure is based on the Muskhelishvili complex variable method of elasticity theory. The force on the dislocation is then derived. It is shown that, in comparison with the two-phase model adopted by Dundurs, the three-phase model allows the dislocation to have equilibrium positions near the fiber.

1 Introduction

Due to the importance of studying the strengthening and hardening mechanisms of various composite materials, a lot of effort has been spent on investigating the interaction between dislocations and inclusions in composite materials during the past three decades. The reason is that a dislocation itself can be used to model a minor defect in composite materials. Furthermore, the dislocation-inclusion interaction solution can be used as a Green's function solution to study crack-inclusion interaction in composites [1]–[3]. Therefore investigation results on dislocation-inclusion interaction are highly demanded to cater for the need of fracture toughness and strength analysis, as well as failure and reliability analysis of various composite materials, especially in metal matrix composites.

A great deal of research work on dislocation-inclusion interaction can be found in the open literature. To name a few, Dundurs and Mura [4] first investigated the interaction between an edge dislocation and a circular inclusion. Following that work, Dundurs and Sendeckyi [5] further solved the problem of an edge dislocation inside a circular inclusion, while the interaction between a screw dislocation and a circular inclusion was studied by Dundurs [6] three years later. Stagni and Lizzio [7] carried out the investigation of an edge dislocation interacting with an elliptic inclusion. The problem for the dislocation inside the elliptic inclusion was analyzed by Warren [8]. Worden and Keer [9] obtained the Green's function for a point load and dislocation in an annular region. More recently, the interaction between a screw dislocation and an elliptical inhomogeneity was investigated by Gong and Meguid [10].

However, all the above-mentioned research work basically involves an isolated inclusion only, i.e., a dislocation interacting with a single inclusion in a homogeneous matrix. For two-phase composite materials, when the inclusion phase has finite concentration, the dislocation interacts not only with the nearest inclusion but also with the surrounding ones. In order to

reflect the mean effect of these interactions, Christensen and Lo [11] and Christensen [12] introduced a three-phase composite cylinder model. In the two dimensional case, the model consists of three concentric regions: the inner circular region representing the inclusion phase, the intermediate annular region representing the pure matrix phase and the outer infinitely extended region representing the composite phase. Based on the three-phase cylinder composite model, Luo and Chen [13] derived the stress field due to an edge dislocation located in the intermediate matrix phase.

The objective of the current study is to investigate the interaction between a screw dislocation and surrounding circular inclusions with the above-mentioned three-phase composite cylinder model. A closed-form analytical solution for the stress field has been obtained. Various numerical examples are given. The force on the dislocation is calculated for different material properties of the inclusions and the matrix. The equilibrium positions of the dislocation are discussed in detail using the evaluated force on the dislocation. The results obtained are compared with those from the two-phase model of Dundurs [6]. It is worth to mention that for the two-phase model the edge dislocation case was solved by Dundurs and Mura [4] first, then the screw dislocation case was solved by Dundurs [6] three years later. For the current three-phase model, as mentioned above, the edge dislocation case was solved by Luo and Chen [13], and the present paper will give the solution for the screw dislocation case.

2 Formulation

The physical problem to be studied is shown in Fig. 1, where the circular fiber-reinforced composite material has been made to be equivalent to a three-phase composite cylinder model [11], [12]: Phase 1 is the circular fiber with elastic properties $\varkappa_1, \mu_1$, occupying the inner region $r \leq a$; Phase 2 is the pure matrix material around the fiber with elastic properties $\varkappa_2, \mu_2$, occupying the intermediate region $a \leq r \leq b$; and Phase 3 is the infinitely extended composite material with elastic properties $\varkappa_3, \mu_3$, occupying the outer region $r \geq b$. A screw dislocation $b = b_z$ is located near the fiber (Phase 1) at a point $(e, 0)$, $a < e < b$. It is worth to mention that through the three-phase model the interactions between the dislocation and the other fibers in the composite are considered by the third phase.

As the formulation is an anti-plane elastic problem, the displacement components in each phase are assumed as:

$$u_x^{(i)} = u_y^{(i)} = 0\,, \qquad u_z^{(i)} = \varphi_i(x, y)\,, \tag{1}$$

for $i = 1, 2, 3$, where $\varphi_i(x, y)$ are some unknown functions (to be evaluated) of x, y. The stress components are thus obtained from Eq. (1) as

$$\sigma_{zx}^{(i)} = \mu_i \frac{\partial \varphi_i}{\partial x}\,, \qquad \sigma_{zy}^{(i)} = \mu_i \frac{\partial \varphi_i}{\partial y}\,, \tag{2}$$

and

$$\sigma_{zz}^{(i)} = \sigma_{xx}^{(i)} = \sigma_{yy}^{(i)} = \sigma_{xy}^{(i)} = 0\,, \tag{3}$$

where μ_i, $i = 1, 2, 3$ are the shear moduli of the respective phases.

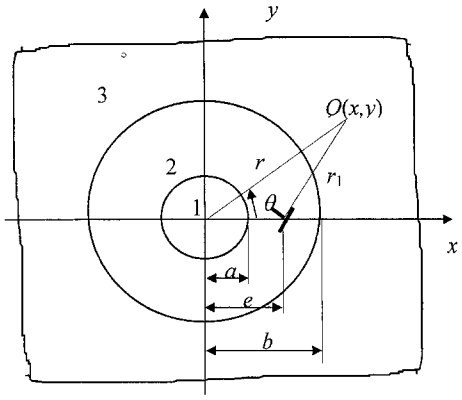

Fig. 1. A screw dislocation in a composite with the three-phase model

Supposing that there is no body force, the stress components given above must satisfy the equilibrium equations

$$\frac{\partial \sigma_{xx}^{(i)}}{\partial x}+\frac{\partial \sigma_{xy}^{(i)}}{\partial y}=\frac{\partial \sigma_{xz}^{(i)}}{\partial z}=0\,,$$

$$\frac{\partial \sigma_{yx}^{(i)}}{\partial x}+\frac{\partial \sigma_{yy}^{(i)}}{\partial y}=\frac{\partial \sigma_{yz}^{(i)}}{\partial z}=0\,, \tag{4}$$

$$\frac{\partial \sigma_{zx}^{(i)}}{\partial x}+\frac{\partial \sigma_{zy}^{(i)}}{\partial y}=\frac{\partial \sigma_{zz}^{(i)}}{\partial z}=0\,,$$

which lead to

$$\frac{\partial^2 \varphi_i}{\partial x^2}+\frac{\partial^2 \varphi_i}{\partial y^2}=0\,. \tag{5}$$

In other words, $\varphi_i(x,y)$ must be harmonic functions of the two variables x, y in the respective phases.

The components of the traction vector acting on the side surface are:

$$T_z^{(i)}=\sigma_{zx}^{(i)}\cos(n,x)+\sigma_{zy}^{(i)}\cos(n,y)=\mu_i\frac{\partial \varphi_i}{\partial n}\,, \tag{6}$$

and

$$T_x^{(i)}=T_y^{(i)}=0\,, \tag{7}$$

where n is the outward normal to the side surface.

Introducing the complex functions $\Phi_i(\Im)$ of the complex variable $\Im=x+iy$, which are defined by

$$\Phi_i(\Im)=\varphi_i+\mathrm{i}\psi_i\,, \tag{8}$$

where $\psi_i(x,y)$ are the conjugate functions of $\varphi_i(x,y)$ and satisfy

$$\frac{\partial \varphi_i}{\partial x}=\frac{\partial \psi_i}{\partial y}\,,\qquad \frac{\partial \varphi_i}{\partial y}=-\frac{\partial \psi_i}{\partial x}\,, \tag{9}$$

it is clear that $\Phi_i(\Im)$ are holomorphic in the respective regions. Hence, the displacement components and the stress components can be written in terms of the complex functions as

$$u_z^{(i)}=\mathrm{Re}\,\Phi_i(\Im) \tag{10}$$

and

$$\sigma_{zy}^{(i)} + \mathrm{i}\sigma_{zx}^{(i)} = \mathrm{i}\mu_i \frac{\partial \Phi_i(\mathfrak{I})}{\partial \mathfrak{I}} . \tag{11}$$

For the current problem, the holomorphic complex functions are taken as

$$\Phi_1(\mathfrak{I}) = \frac{b_z}{2\pi}\left[\Phi_0(\mathfrak{I}) + \sum_{k=0}^{\infty}(a_k' + ib_k')\,\mathfrak{I}^k\right], \tag{12}$$

$$\Phi_2(\mathfrak{I}) = \frac{b_z}{2\pi}\left[\Phi_0(\mathfrak{I}) + \sum_{k=-\infty}^{\infty}(a_k'' + ib_k'')\,\mathfrak{I}^k\right], \tag{13}$$

$$\Phi_3(\mathfrak{I}) = \frac{b_z}{2\pi}\left[\Phi_0(\mathfrak{I}) + \sum_{k=-\infty}^{1}(a_k''' + ib_k''')\,\mathfrak{I}^k\right], \tag{14}$$

in the three phases, respectively, where

$$\Phi_0(\mathfrak{I}) = \frac{}{}\mathrm{i}\log(\mathfrak{I} - e) . \tag{15}$$

Combining Eqs. (12)–(14), we have

$$\varphi_1 = \frac{b_z}{2\pi}\left[\varphi_0 + a_0' + \sum_{k=1}^{\infty}(a_k'\cos k\theta - b_k'\sin k\theta)\,r^k\right], \tag{16}$$

$$\varphi_2 = \frac{b_z}{2\pi}\left[\varphi_0 + a_0'' + \sum_{k=1}^{\infty}(a_k''\cos k\theta - b_k''\sin k\theta)\,r^k + \sum_{k=1}^{\infty}(a_{-k}''\cos k\theta + b_{-k}''\sin k\theta)\,r^{-k}\right], \tag{17}$$

$$\varphi_3 = \frac{b_z}{2\pi}\left[\varphi_0 + \sum_{k=1}^{\infty}(a_{-k}'''\cos k\theta + b_{-k}'''\sin k\theta)\,r^{-k}\right] \tag{18}$$

with

$$\varphi_0 = \mathrm{Re}\,\Phi_0 . \tag{19}$$

The boundary conditions are:

at $r = a$,

$$u_z^{(1)} = u_z^{(2)}, \qquad T_z^{(1)} = T_z^{(2)}; \tag{20}$$

at $r = b$,

$$u_z^{(2)} = u_z^{(3)}, \qquad T_z^{(2)} = T_z^{(3)} . \tag{21}$$

Using Eqs. (1) and (6), the boundary conditions are rewritten as

$$\varphi_1|_{r=a} = \varphi_2|_{r=a}, \qquad \frac{\mu_1}{\mu_2}\frac{\partial\varphi_1}{\partial r}\bigg|_{r=a} = \frac{\partial\varphi_2}{\partial r}\bigg|_{r=a}, \tag{22.1}$$

$$\varphi_2|_{r=b} = \varphi_3|_{r=b}, \qquad \frac{\partial\varphi_2}{\partial r}\bigg|_{r=b} = \frac{\mu_3}{\mu_2}\frac{\partial\varphi_3}{\partial r}\bigg|_{r=b} . \tag{22.2}$$

When $|\mathfrak{I}| < e$,

$$\log(\mathfrak{I} - e) = \log e + \mathrm{i}\pi - \sum_{k=1}^{\infty} \frac{\mathfrak{I}^k}{ke^k}, \tag{23}$$

$$\frac{1}{\mathfrak{I} - e} = -\sum_{k=0}^{\infty} e^{k+1}\mathfrak{I}^k, \tag{24}$$

and when $|\mathfrak{I}| > e$, we have

$$\log(\mathfrak{I} - e) = \log \mathfrak{I} - \sum_{k=1}^{\infty} \frac{e^k}{k\mathfrak{I}^k}, \tag{25}$$

$$\frac{1}{\mathfrak{I} - e} = \sum_{k=0}^{\infty} e^k \frac{1}{\mathfrak{I}^{k+1}}. \tag{26}$$

Therefore, φ_0 and $\dfrac{\partial \varphi_0}{\partial r}$ can be rewritten as:

for $r < e$:

$$\varphi_0 = \pi - \sum_{k=1}^{\infty} \frac{r^k}{ke^k} \sin k\theta, \tag{27}$$

$$\frac{\partial \varphi_0}{\partial r} = -\sum_{k=1}^{\infty} \frac{r^{k-1}}{e^k} \sin k\theta, \tag{28}$$

and for $r > e$:

$$\varphi_0 = \theta + \sum_{k=1}^{\infty} \frac{e^k}{kr^k} \sin k\theta, \tag{29}$$

$$\frac{\partial \varphi_0}{\partial r} = -\sum_{k=1}^{\infty} \frac{e^k}{r^{k+1}} \sin k\theta. \tag{30}$$

Furthermore, in Eq. (29) $\theta(-\pi \le \theta \le \pi)$ can be expressed by

$$\theta = 2\sum_{k=1}^{\infty} \frac{(-1)^{k-1}}{k} \sin k\theta. \tag{31}$$

Recalling Eq. (8), and writing $\mathfrak{I}$ as $\mathfrak{I} = r(\cos\theta + \mathrm{i}\sin\theta)$, by comparing the coefficients of $\sin k\theta$ and $\cos k\theta$, the boundary conditions lead to the following linear equations which determine the coefficients $a_0', a_0'', a_k', a_k'', a_{-k}'', a_{-k}''', b_k', b_k'', b_{-k}'', b_{-k}'''$ with $k = 1, 2, \ldots$:

$$\begin{aligned}
&a_0' = a_0'', a_k' = a_k'' + a_{-k}''/a^{2k}, \qquad b_k' = b_k'' - b_{-k}''/a^{2k}, \\
&\frac{\mu_1}{\mu_2} a_k' = a_k'' - a_{-k}''/a^{2k}, \qquad \frac{\mu_1}{\mu_2} b_k' = b_k'' + b_{-k}''/a^{2k} + \frac{1}{ke^k}\left(1 - \frac{\mu_1}{\mu_2}\right), \\
&a_0'' = 0, \qquad a_k'' + a_{-k}''/b^{2k} = a_{-k}'''/b^{2k}, \qquad b_k'' - b_{-k}''/b^{2k} = -b_{-k}'''/b^{2k}, \\
&a_k'' - a_{-k}''/b^{2k} = -\frac{\mu_3}{\mu_2} a_{-k}'''/b^{2k}, \qquad b_k'' + b_{-k}''/b^{2k} - \frac{\mu_3}{\mu_2} b_{-k}'''/b^{2k} = \left(\frac{\mu_3}{\mu_2} - 1\right) \frac{e^k}{kb^{2k}}.
\end{aligned} \tag{32}$$

Solving the above equations, we obtain

$$a_0' = a_0'' = a_k' = a_k'' = a_{-k}'' = a_{-k}''' = 0\,,$$

$$b_k' = \frac{-\left(\frac{\mu_1}{\mu_2}-1\right)\left[(1+a^{2k})+\frac{\mu_3}{\mu_2}(1-\alpha^{2k})\right]+2\left(\frac{\mu_3}{\mu_2}-1\right)\left(\frac{e}{b}\right)^{2k}}{ke^k\left[(1+\alpha^{2k})\left(\frac{\mu_1}{\mu_2}+\frac{\mu_3}{\mu_2}\right)+(1-\alpha^{2k})\left(1+\frac{\mu_3}{\mu_2}\frac{\mu_1}{\mu_2}\right)\right]}\,,$$

$$b_k'' = \frac{\alpha^{2k}\left(\frac{\mu_1}{\mu_2}-1\right)\left(\frac{\mu_3}{\mu_2}-1\right)+\left(\frac{\mu_1}{\mu_2}+1\right)\left(\frac{\mu_3}{\mu_2}-1\right)\left(\frac{e}{b}\right)^{2k}}{ke^k\left[(1+\alpha^{2k})\left(\frac{\mu_1}{\mu_2}+\frac{\mu_3}{\mu_2}\right)+(1-\alpha^{2k})\left(1+\frac{\mu_3}{\mu_2}\frac{\mu_1}{\mu_2}\right)\right]}\,, \tag{33}$$

$$b_{-k}'' = \frac{a^{2k}\left(\frac{\mu_1}{\mu_2}-1\right)\left(\frac{\mu_3}{\mu_2}+1\right)+a^{2k}\left(\frac{\mu_1}{\mu_2}-1\right)\left(\frac{\mu_3}{\mu_2}-1\right)\left(\frac{e}{b}\right)^{2k}}{ke^k\left[(1+\alpha^{2k})\left(\frac{\mu_1}{\mu_2}+\frac{\mu_3}{\mu_2}\right)+(1-\alpha^{2k})\left(1+\frac{\mu_3}{\mu_2}\frac{\mu_1}{\mu_2}\right)\right]}\,,$$

$$b_{-k}''' = \frac{2a^{2k}\left(\frac{\mu_1}{\mu_2}-1\right)-a^{2k}\left(\frac{\mu_1}{\mu_2}+1\right)\left(\frac{\mu_3}{\mu_2}-1\right)\left(\frac{e}{a}\right)^{2k}+a^{2k}\left(\frac{\mu_1}{\mu_2}-1\right)\left(\frac{\mu_3}{\mu_2}-1\right)\left(\frac{e}{b}\right)^{2k}}{ke^k\left[(1+\alpha^{2k})\left(\frac{\mu_1}{\mu_2}+\frac{\mu_3}{\mu_2}\right)+(1-\alpha^{2k})\left(1+\frac{\mu_3}{\mu_2}\frac{\mu_1}{\mu_2}\right)\right]}\,,$$

where

$$\alpha = \frac{a}{b}\,. \tag{34}$$

3 Stress field

The stress components in the regions 1, 2 and 3 can be calculated using Eq. (11) with the aid of Eqs. (12) to (14), given by

$$\sigma_{zy}^{(1)} = \frac{\mu_1 b_z}{2\pi}\left[\frac{x-e}{(x-e)^2+y^2}-\sum_{k=1}^{\infty} r^{k-1}k\cos(k-1)\theta b_k'\right],$$
$$\sigma_{zx}^{(1)} = \frac{\mu_1 b_z}{2\pi}\left[\frac{-y}{(x-e)^2+y^2}-\sum_{k=1}^{\infty} r^{k-1}k\sin(k-1)\theta b_k'\right], \tag{35}$$

$$\sigma_{zy}^{(2)} = \frac{\mu_2 b_z}{2\pi}\left[\frac{x-e}{(x-e)^2+y^2}-\sum_{k=1}^{\infty} r^{k-1}k\cos(k-1)\theta b_k''+\sum_{k=1}^{\infty}\frac{\cos(k+1)\theta}{r^{k+1}}kb_{-k}''\right],$$
$$\sigma_{zx}^{(2)} = \frac{\mu_2 b_z}{2\pi}\left[\frac{-y}{(x-e)^2+y^2}-\sum_{k=1}^{\infty} r^{k-1}k\sin(k-1)\theta b_k''-\sum_{k=1}^{\infty}\frac{\sin(k+1)\theta}{r^{k+1}}kb_{-k}''\right], \tag{36}$$

$$\sigma_{zy}^{(3)} = \frac{\mu_3 b_z}{2\pi}\left[\frac{x-e}{(x-e)^2+y^2}+\sum_{k=1}^{\infty}\frac{\cos(k+1)\theta}{r^{k+1}}kb_{-k}'''\right],$$
$$\sigma_{zx}^{(3)} = \frac{\mu_3 b_z}{2\pi}\left[\frac{-y}{(x-e)^2+y^2}-\sum_{k=1}^{\infty}\frac{\sin(k+1)\theta}{r^{k+1}}kb_{-k}'''\right]. \tag{37}$$

From Eq. (33) and the above equations, we find that when $\mu_3/\mu_2 = 1$, the solutions can be completely reduced to those of the two-phase model given by Dundurs [6] , a screw dislocation embedded in an infinite elastic material with a circular inclusion.

4 Force on dislocation

When $Q(x, y)$ is on the x-axis, from Eqs. (36) and (37) we have

$$\sigma_{zy}^{(2)}(x,0) = \frac{\mu_2 b_z}{2\pi}\left[\frac{1}{x-e} - \sum_{k=1}^{\infty} x^{k-1} k b_k'' + \sum_{k=1}^{\infty} \frac{1}{x^{k+1}}\, k b_{-k}''\right], \qquad \sigma_{zx}^{(2)} = 0, \tag{38}$$

$$\sigma_{zy}^{(3)}(x,0) = \frac{\mu_3 b_z}{2\pi}\left[\frac{1}{x-e} + \sum_{k=1}^{\infty} \frac{1}{x^{k+1}}\, k b_{-k}'''\right], \qquad \sigma_{zx}^{(3)} = 0. \tag{39}$$

The strain energy W is computed as the work required to reject the dislocation in the materials, thus,

$$W = \frac{1}{2}\, b_z \left[\int_{e+r_0}^{b} \sigma_{zy}^{(2)}(x,0)\, dx + \int_{b}^{R} \sigma_{zy}^{(3)}(x,0)\, dx\right], \tag{40}$$

where R is the distance corresponding to the material size and r_0 is the core radius of the dislocation. One may take $R \to \infty$ and $r_0 \to 0$ for all terms in the integral that converge at those limits. Evaluating Eq. (40) by use of Eqs. (38) and (39), we find

$$W = \frac{\mu_2 b_z^2}{4\pi}\left\{\log\frac{b-e}{r_0} + \frac{\mu_3}{\mu_2}\log\frac{R}{b-e} + \sum_{k=1}^{\infty}\left[(e^k - b^k)\, b_k'' + \left(\frac{1}{e^k} - \frac{1}{b^k}\right) b_{-k}'' + \frac{\mu_3}{\mu_2}\frac{1}{b^k}\, b_{-k}'''\right]\right. \tag{41.1}$$

or

$$\begin{aligned} W = \frac{\mu_2 b_z^2}{4\pi}\left\{\log\frac{b-e}{r_0} + \frac{\mu_3}{\mu_2}\log\frac{R}{b-e} + \sum_{k=1}^{\infty}\left[\left(\frac{\alpha^{2k}}{k} - \frac{\alpha^k}{k\beta^k}\right) A_{1k} + \left(\frac{\alpha^{2k}\beta^{2k}}{k} - \frac{\alpha^k\beta^k}{k}\right) A_{2k}\right.\right. \\ \left.\left. + \left(\frac{1}{k\beta^{2k}} - \frac{\alpha^k}{k\beta^k}\right) A_{3k} + \left(\frac{\alpha^{2k}}{k} - \frac{\alpha^{3k}\beta^k}{k}\right) A_{4k} + \frac{\alpha^k B_{1k}}{k\beta^k} - \frac{B_{2k}}{k}\,\alpha^k\beta^k + \frac{B_{3k}}{k}\,\alpha^{3k}\beta^k\right]\right\}, \end{aligned} \tag{41.2}$$

where

$$\beta = \frac{e}{a}, \qquad A_{1k} = \frac{\left(\frac{\mu_1}{\mu_2} - 1\right)\left(\frac{\mu_3}{\mu_2} - 1\right)}{(1+\alpha^{2k})\left(\frac{\mu_1}{\mu_2} + \frac{\mu_3}{\mu_2}\right) + (1-\alpha^{2k})\left(1 + \frac{\mu_3}{\mu_2}\frac{\mu_1}{\mu_2}\right)}, \tag{42.1}$$

$$A_{2k} = \frac{\left(\frac{\mu_1}{\mu_2} + 1\right)\left(\frac{\mu_3}{\mu_2} - 1\right)}{(1+\alpha^{2k})\left(\frac{\mu_1}{\mu_2} + \frac{\mu_3}{\mu_2}\right) + (1-\alpha^{2k})\left(1 + \frac{\mu_3}{\mu_2}\frac{\mu_1}{\mu_2}\right)}, \tag{42.2}$$

$$A_{3k} = \frac{\left(\frac{\mu_1}{\mu_2} - 1\right)\left(\frac{\mu_3}{\mu_2} - 1\right)}{(1+\alpha^{2k})\left(\frac{\mu_1}{\mu_2} + \frac{\mu_3}{\mu_2}\right) + (1-\alpha^{2k})\left(1 + \frac{\mu_3}{\mu_2}\frac{\mu_1}{\mu_2}\right)}, \tag{42.3}$$

$$A_{4k} = \frac{\left(\frac{\mu_1}{\mu_2} - 1\right)\left(\frac{\mu_3}{\mu_2} - 1\right)}{(1+\alpha^{2k})\left(\frac{\mu_1}{\mu_2} + \frac{\mu_3}{\mu_2}\right) + (1-\alpha^{2k})\left(1 + \frac{\mu_3}{\mu_2}\frac{\mu_1}{\mu_2}\right)}, \tag{42.4}$$

$$B_{1k} = \frac{2\left(\frac{\mu_1}{\mu_2} - 1\right)\frac{\mu_3}{\mu_2}}{(1+\alpha^{2k})\left(\frac{\mu_1}{\mu_2} + \frac{\mu_3}{\mu_2}\right) + (1-\alpha^{2k})\left(1 + \frac{\mu_3}{\mu_2}\frac{\mu_1}{\mu_2}\right)}, \tag{42.5}$$

$$B_{2k} = \frac{\left(\frac{\mu_1}{\mu_2} + 1\right)\left(\frac{\mu_3}{\mu_2} - 1\right)\frac{\mu_3}{\mu_2}}{(1+\alpha^{2k})\left(\frac{\mu_1}{\mu_2} + \frac{\mu_3}{\mu_2}\right) + (1-\alpha^{2k})\left(1 + \frac{\mu_3}{\mu_2}\frac{\mu_1}{\mu_2}\right)}, \tag{42.6}$$

$$B_{3k} = \frac{\left(\frac{\mu_1}{\mu_2} - 1\right)\left(\frac{\mu_3}{\mu_2} - 1\right)\frac{\mu_3}{\mu_2}}{(1+\alpha^{2k})\left(\frac{\mu_1}{\mu_2} + \frac{\mu_3}{\mu_2}\right) + (1-\alpha^{2k})\left(1 + \frac{\mu_3}{\mu_2}\frac{\mu_1}{\mu_2}\right)}. \tag{42.7}$$

The force on the dislocation is purely radial, it is defined as

$$F = -\frac{\partial W}{\partial e} = -\frac{1}{a}\frac{\partial W}{\partial \beta}. \tag{43}$$

From Eq. (41), we obtain

$$F = -\frac{\mu_2 b_z^2}{4\pi a}\sum_{k=1}^{\infty}\left[\left(\frac{\mu_3}{\mu_2} - 1\right)\frac{\alpha}{1-\alpha\beta} + \frac{\alpha^k A_{1k}}{\beta^{k+1}} + \left(2\alpha^{2k}\beta^{2k-1} - \alpha^k\beta^{k-1}\right)A_{2k} + \left(\frac{\alpha^k}{\beta^{k+1}} - \frac{2}{\beta^{2k+1}}\right)A_{3k} - \alpha^{3k}\beta^{k-1}A_{4k} - \frac{\alpha^k B_{1k}}{\beta^{k+1}} - \alpha^k\beta^{k-1}B_{2k} + \alpha^{3k}\beta^{k-1}B_{3k}\right]. \tag{44}$$

5 Numerical examples and discussion

It has been seen that in the three-phase composite cylinder model the force on the dislocation is a rather complicated function of various parameters, such as the dislocation location $\beta = e/a$, the characteristic length $\alpha = a/b$, and the material properties of the inclusion and the matrix. As a result, it becomes quite difficult to determine the equilibrium position of a dislocation where the force F vanishes.

However, from our numerical calculations, we find that when the dislocation is close to the fiber-matrix interface ($\beta \to 1$), the term containing A_{3k} in Eq. (44) is dominant, and when the dislocation is close to the matrix-composite interface ($\beta\alpha \to 1$), the first term and the term containing B_{2k} in Eq. (44) are dominant. Thus, we have the following set of criteria: When $\mu_1/\mu_2 < 1$, the dislocation is attracted by the fiber phase, and repelled by it when $\mu_1/\mu_2 > 1$; when $\mu_3/\mu_2 > 1$, the dislocation is repelled by the composite phase, and attracted by it when $\mu_3/\mu_2 < 1$. Hence, if $\mu_1/\mu_2 > 1$ and $\mu_3/\mu_2 > 1$, the dislocation will have at least one stable equilibrium position in $a \le e \le b$; if $\mu_1/\mu_2 < 1$ and $\mu_3/\mu_2 < 1$, the dislocation will have at least one unstable equilibrium position in $a \le e \le b$. This conclusion is quite different from

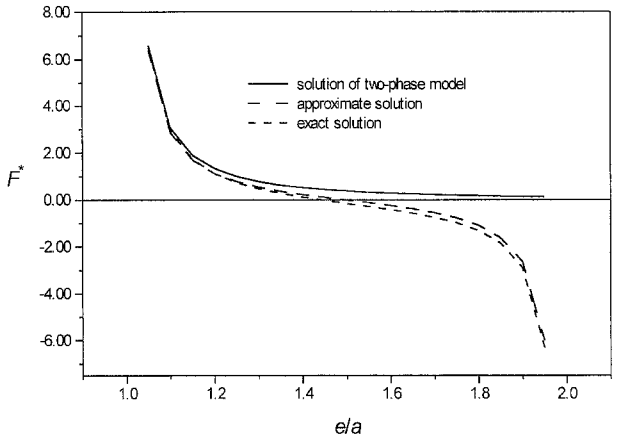

Fig. 2. Variation of the normalized force on the dislocation with the distance $\beta = e/a$ for $\mu_1 = 20\,\mu_2$, $\mu_3 = 8\,\mu_2$, $a/b = 0.5$

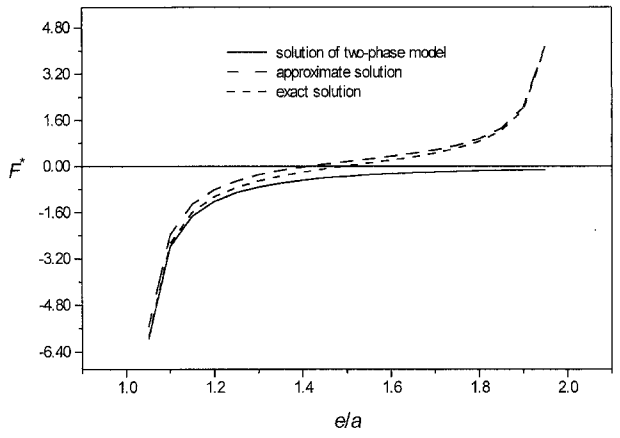

Fig. 3. Variation of the normalized force on the dislocation with the distance $\beta = e/a$ for $\mu_1 = 0.1\,\mu_2$, $\mu_3 = 0.3\,\mu_2$, $a/b = 0.5$

that of the two-phase model by Dundurs [6] , where no equilibrium position is possible for the dislocation.

If the ratio b/a is not fairly large, we can use the following approximation to estimate the force on the dislocation:

$$F = -\frac{\mu_2 b_z^2}{4\pi a}\sum_{k=1}^{\infty}\left[\left(\frac{\alpha^k}{\beta^{k+1}} - \frac{2}{\beta^{2k+1}}\right)A_{3k} + \left(\frac{\mu_3}{\mu_2} - 1\right)\frac{\alpha}{1-\alpha\beta}\right]. \tag{46}$$

Let

$$F^* = \frac{F}{\mu_2 b_z^2/2\pi a}, \tag{47}$$

then

$$\frac{\partial F^*}{\partial \beta} = -\sum_{k=1}^{\infty}\left[\left(\frac{2k+1}{\beta^{2k+2}} - \frac{(k+1)\,\alpha^k}{\beta^{k+2}}\right)A_{3k} + \left(\frac{\mu_3}{\mu_2} - 1\right)\frac{\alpha^2}{(1-\alpha\beta)^2}\right]. \tag{48}$$

Noting that $1 < \beta < 1/\alpha$, thus if $\mu_1/\mu_2 > 1$ and $\mu_3/\mu_2 > 1$, F^* monotonically decreases; and if $\mu_1/\mu_2 < 1$ and $\mu_3/\mu_2 < 1$, F^* monotonically increases. Therefore, if $\mu_1/\mu_2 > 1$ and

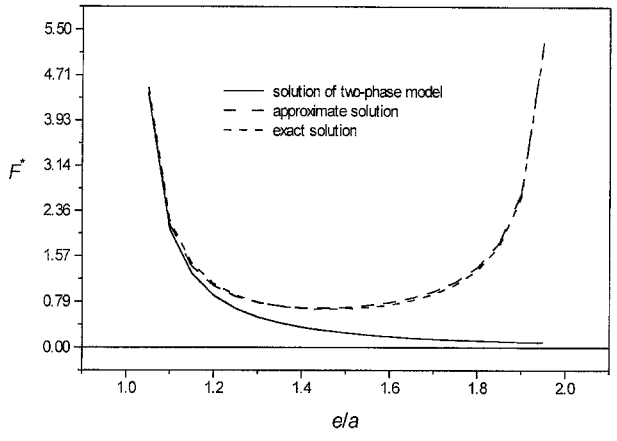

Fig. 4. Variation of the normalized force on the dislocation with the distance $\beta = e/a$ for $\mu_1 = 4\,\mu_2$, $\mu_3 = 0.2\,\mu_2$, $a/b = 0.5$

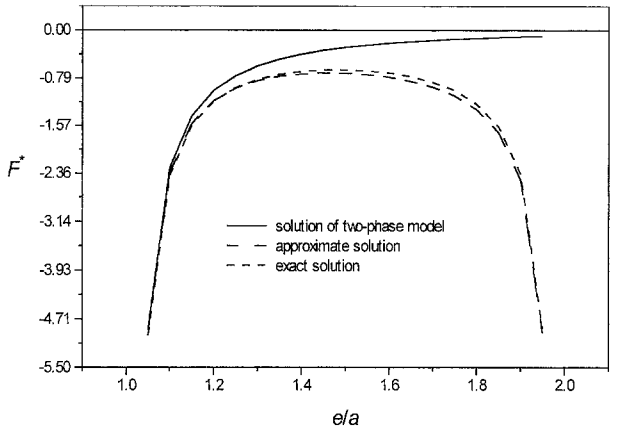

Fig. 5. Variation of the normalized force on the dislocation with the distance $\beta = e/a$ for $\mu_1 = 0.2\,\mu_2$, $\mu_3 = 4\,\mu_2$, $a/b = 0.5$

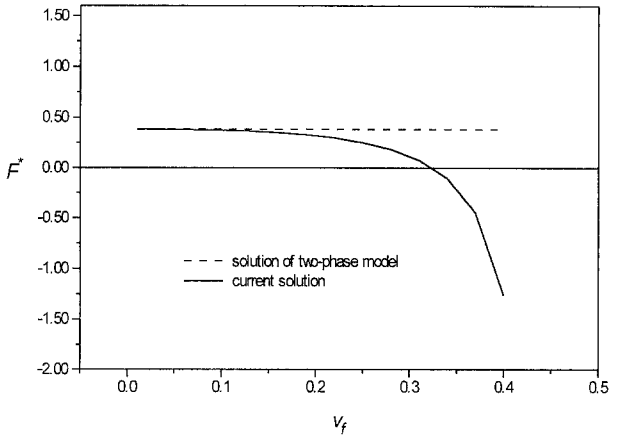

Fig. 6. The normalized force on the dislocation versus the volume fraction of the fiber in a fiber-reinforced composite with $\mu_1 = 23\,\mu_2$, $\nu_1 = 0.3$, $\nu_2 = 0.35$, $e/b = 1.5$

$\mu_3/\mu_2 > 1$, there is only one stable equilibrium position, and if $\mu_1/\mu_2 < 1$ and $\mu_3/\mu_2 < 1$, there is only one unstable equilibrium position.

The normalized force F^* versus the normalized distance $\beta = e/a$ is depicted in Fig. 2 to Fig. 5 for the four particular material combinations characterized by $(\mu_1/\mu_2 > 1, \mu_3/\mu_2 > 1)$, $(\mu_1/\mu_2 < 1, \mu_3/\mu_2 < 1)$, $(\mu_1/\mu_2 > 1, \mu_3/\mu_2 < 1)$ and $(\mu_1/\mu_2 < 1, \mu_3/\mu_2 > 1)$, respectively.

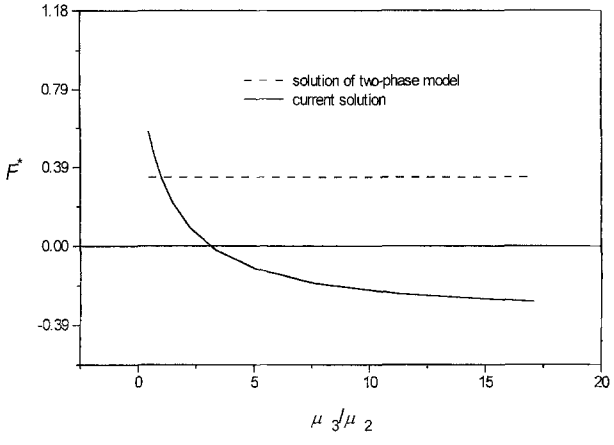

Fig. 7. Normalized force on the dislocation versus shear modulus μ_3/μ_2 in a real three-phase cylinder with $\mu_1 = 10\,\mu_2$, $e/b = 1.5$, $a/b = 0.5$

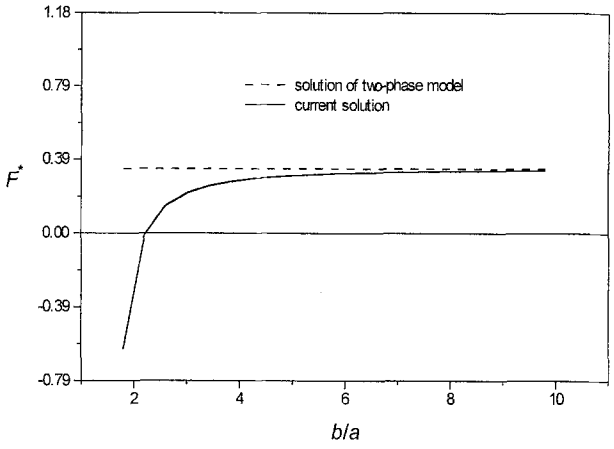

Fig. 8. Normalized force on the dislocation versus b/a in a real three-phase cylinder with $\mu_1 = 10\,\mu_2$, $\mu_3 = 8\,\mu_2$, $e/b = 1.5$

Both the exact solution calculated by Eq. (44) and the approximate solution by Eq. (46) are displayed. It is seen that the approximate solution gives a very good result. In each figure, the corresponding result of the two-phase model from Dundurs [6] is also given. The present three-phase model shows a stable equilibrium position in Fig. 2 and an unstable equilibrium position in Fig. 3, which is totally different from the two-phase model [6] where no equilibrium position is possible for the dislocation. However, for the material property combinations given in Figs. 4 and 5, neither the solution of the present three-phase model nor that of the two-phase model has any equilibrium position through the whole intervals.

In order to examine the influence of the volume fraction of the fibers on the force of the dislocation in a fiber-reinforced composite, the following materials are used for numerical examples: $\mu_1/\mu_2 = 23$, $\nu_1 = 0.3$, $\nu_2 = 0.35$, and the elastic constants of the composite, namely, the outer phase, are evaluated according to Christensen [12]. In Fig. 6, the force on the dislocation F^* is plotted as a function of the volume fraction ν_f. It is observed that the force decreases with increasing fiber concentration, when the fibers are much "harder" than the matrix.

As it is emphasized, the main objective of the current study is to investigate the dislocation-inclusions interaction in fiber-reinforced composite materials. It is worth to mention that a "by-product" application of the paper is that the analytical solution obtained can also be

used to study the dislocation behavior in a real three-phase cylinder. In other words, if the Phase 3 in Fig. 1 is not the equivalent composite, but the third real different material, the result obtained in the current study can be directly applied. Here two numerical examples are given. The force F^* versus the shear modulus μ_3/μ_2 is plotted in Fig. 7 for $\mu_1/\mu_2 = 10$, $a/b = 0.5$ at the point $\beta = 1.5$. The figure shows that when the rigidity of the outer phase (Phase 3) is low, the dislocation is repelled by the harder centre inclusion; when the rigidity of the outer phase becomes high, the dislocation is repelled by the outer phase. In order to examine the influence of the geometry on the force on the dislocation, F^* is plotted versus b/a in Fig. 8 for $\mu_1 7\mu_2 = 10$, $\mu_3/\mu_2 = 8$ at the point $\beta = 1.5$. As expected, with increasing value of b/a, the solution slowly approaches that of the two-phase case given by Dundurs [6].

References

[1] Erdogan, F., Gupta, G. D., Ratwani M.: Interaction between a circular inclusion and an arbitrarily oriented crack. ASME J. Appl. Mech. **41,** 1007–1013 (1974).
[2] Nisitani, H., Chen, D. H., Saimoto, A.: Interaction between an elliptic inclusion and a crack. Proc. Int. Conference on Computer-Aided Assessment and Control, Computational Mechanics Inc, MA, USA, **4,** pp. 325–332 (1996).
[3] Xiao, Z. M., Chen, B. J.: Stress intensity factor for a Griffith crack interacting with a coated inclusion. Int. J. Fract. (in press).
[4] Dundurs, J., Mura, T.: Interaction between an edge dislocation and a circular inclusion. J. Mech. Phys. Solids **12,** 177–189 (1964).
[5] Dundurs, J., Sendeckyi, G. P.: Edge dislocation inside a circular inclusion. J. Mech. Phys. Solids **13,** 141–147 (1965).
[6] Dundurs, J.: On the interaction of a screw dislocation with inhomogeneities. Recent Adv. Engng Sci. **2,** 223–233 (1967).
[7] Stagni, L., Lizzio, R.: Shape effects in the interaction between an edge dislocation and an elliptic inclusion. J. Appl. Phys. **A30,** 217–221 (1993).
[8] Warren, W. E.: The edge dislocation inside an elliptic inclusion. Mech. Mat. **2,** 319–330 (1983).
[9] Worden, R. E., Keer, L. M.: Green's functions for a point load and dislocation in an annular region. ASME J. Appl. Mech. **58,** 954–959 (1991).
[10] Gong, S. X., Meguid, S. A.: Screw dislocation interacting with an elastic elliptical inhomogeneity. Int. J. Engng Sci. **32,** 1221–1228 (1994).
[11] Christensen, R. M., Lo, K. H.: Solution for effective shear properties in three-phase sphere and cylinder models. J. Mech. Phys. Solids **27,** 315–330 (1979).
[12] Christensen, R. M.: Mechanics of composite materials. New York: Wiley 1979.
[13] Luo, H. A., Chen, Y.: An edge dislocation in a three-phase composite cylinder model. ASME J. Appl. Mech. **58,** 75–86 (1991).

Authors' address: Z. M. Xiao and B. J. Chen, School of Mechanical and Production Engineering, Nanyang Technological University, Nanyang Avenue, Singapore 639798, Republic of Singapore (E-mail: mzxiao@ntu.edu.sg)